P170526

Climate Change Modelling Report

Assessment of Suitable Flood Mitigation Measures (based on Dukniskhevi River Extreme Flood Analysis) in Tbilisi, Georgia

CTCN REFERENCE NUMBER: 2016000043

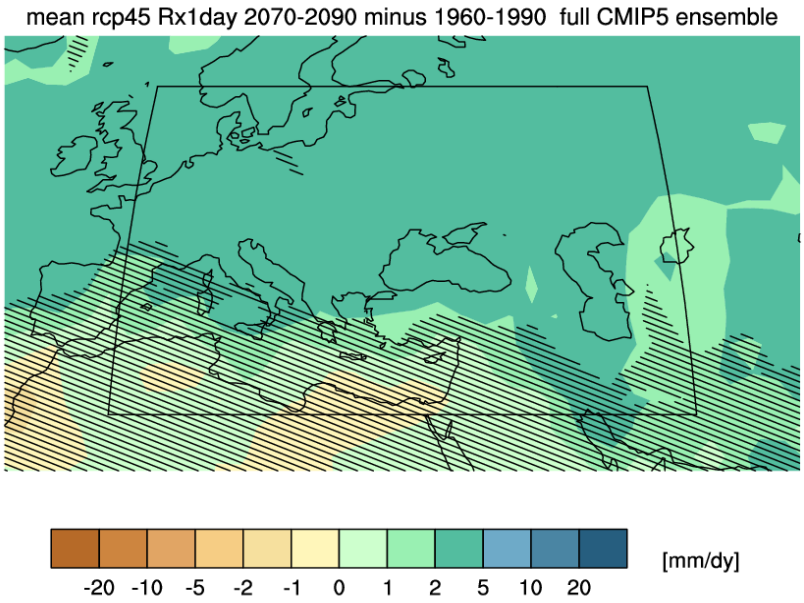

Document Information	
Date	22.04.2018
HYDROC project no.	P170526
HYDROC responsible	Juan Fernandez
Client	CTC-N/UNIDO
Reference No.	2016000043
Project No.	
Credit No.	

Contact
HYDROC GmbH
Siegum 4
24960 Siegum
Germany

Tel - +49 172 450 91 49
Email - info@hydroc.de

Table of Contents

Table of Figures

Table of Tables

List of Abbreviations

CTC-N	Climate Technology Centre and Network
DEM	Digital Elevation Model
ED	Environment and Development
EMA	Emergency Management Agency
FEMA	Federal Emergency Management Agency
GIS	Geographical Information System
GPM	Global Precipitation Measurement
HEC	Hydrologic Engineering Center
MPE	Multisensor Precipitation Estimate
NEA	National Environment Agency
RMS	Root Mean Square Error
SCS	Soil Conservation Service
TRMM	Tropical Rainfall Measuring Mission
UNFCCC	United Nations Framework Convention on Climate Change
WFD	Water Framework Directive

1 Overview

The climate change scenarios are intended to provide information on the changing likelihood of high intensity rainfall events in the region of interest over the next 100 years. To this end, firstly a survey of projected change in the rainfall climate has been carried out; secondly, return periods for large rainfall events have been estimated.

All results are based on the CMIP5 archive of climate model outputs, with local rain gauge data used for bias correction and scaling.

2 Time horizons

The following time slices will be considered:

- 2030 – 2050 (near term change)
- 2070 – 2090 (long term change)

The rationale for choosing 2030-2050 to describe 'near term' climate change is that closer to the present day, it is difficult or impossible to distinguish signals of change from natural year-to-year variation in the weather.

3 CO_2 concentration scenarios

Lack of knowledge of future emissions is a key source of uncertainty in climate projections. The CMIP5 approach is to carry out climate model simulations for a range of greenhouse gas concentration trajectories, described by Representative Concentration Pathways (RCPs) (Van Vuuren et al, 2011). Although the RCPs are based on CO2 concentration, rather than emissions, the two are closely related (**Figure 1** and **Figure 2**).

To give an idea of uncertainty related to future emissions, the following RCPs are considered:

- RCP 2.6: Low emissions scenario, with CO_2 emissions stabilizing and declining after ~2020.
- RCP 4.5: Medium emissions scenario, with CO_2 emissions gradually increasing until ~2040 and then declining.
- RCP 8.5: High emissions scenario, with CO_2 emissions increasing at close to present day rates throughout the 21st Century.

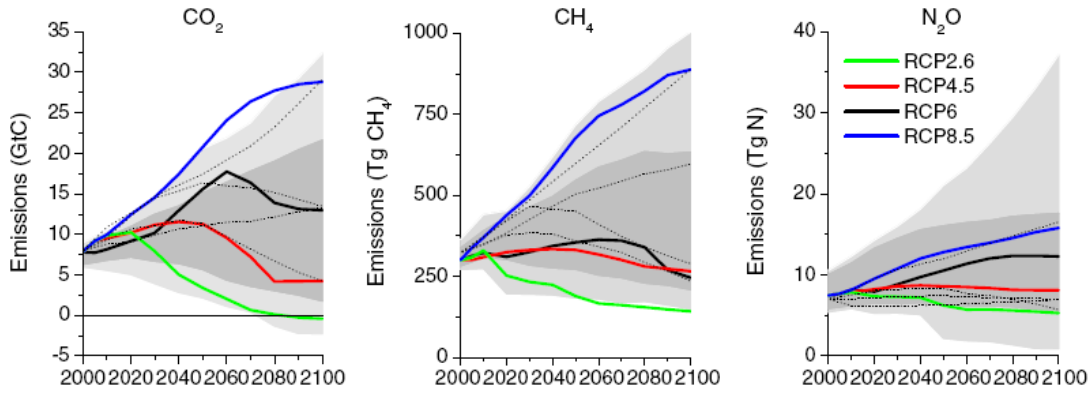

Figure 1: *Emissions of the main greenhouse gases across the RCPs. Grey area indicates the 98th and 90th percentiles (light/dark grey) of the literature. The dotted lines indicate four of the SRES marker scenarios. (from van Vuuren et.al. 2011)*

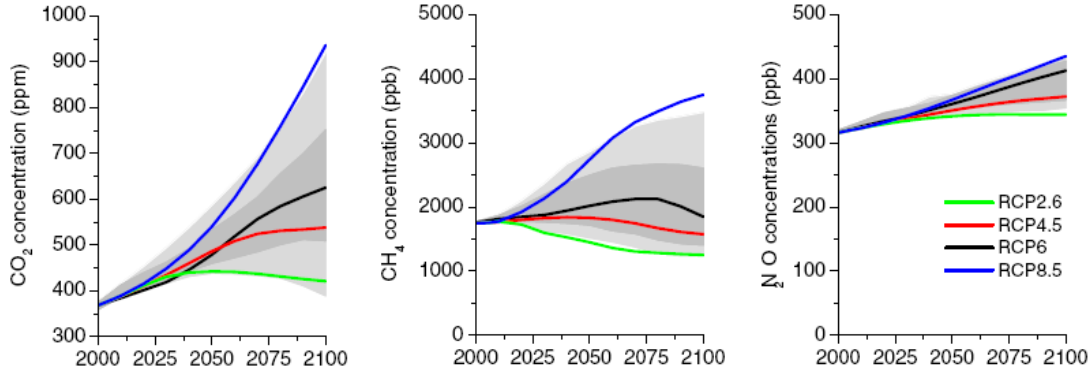

Figure 2: *Trends in concentrations of greenhouse gases (van Vuuren 2011). Grey area indicates the 98th and 90th percentiles (light/dark grey) of a recently published climate change control scenario study (Clarke et al. 2009).*

4 Climate models

In a modification to the original proposed methodology (see Deliverable 3 report), the study was extended from 17 models to the 29 listed in the table below. Using a large ensemble multi-model, enabled us to isolate changes in extremes within short time series of noisy data.

All models were regridded to a common 2.5^0 grid, and the results were downscaled based on the Kojoro raingauge data.

Table 1: Native spatial resolution of climate models used in the analyses

Model	**Longitude resolution**	**Latitude resolution**
ACCESS1.0	1.25	1.875
BCC-CSM1.1	2.7906	2.8125
BCC-CSM1.1(m)	2.7906	2.8125
CCSM4	0.9424	1.25
CMCC-CM	0.7484	0.75
CMCC-CMS	3.7111	3.75
CNRM-CM5	1.4008	1.40625
CNRM-CM5-2	1.4008	1.40625
CSIRO-Mk3.6.0	1.8653	1.875
CanESM2	2.7906	2.8125
EC-EARTH	1.1215	1.125
GFDL-CM3	2	2.5
GFDL-ESM2G	2.0225	2
GFDL-ESM2M	2.0225	2.5
GISS-E2-R	2	2.5
GISS-E2-R-CC	2	2.5
HadGEM2-CC	1.25	1.875
HadGEM2-ES	1.25	1.875
INM-CM4	1.5	2
IPSL-CM5A-LR	1.8947	3.75
IPSL-CM5A-MR	1.2676	2.5

IPSL-CM5B-LR	1.8947	3.75
MIROC-ESM	2.7906	2.8125
MIROC5	1.4008	1.40625
MPI-ESM-LR	1.8653	1.875
MPI-ESM-MR	1.8653	1.875
MPI-ESM-P	1.8653	1.875
MRI-CGCM3	1.12148	1.125
NorESM1-M	1.8947	2.5

5 Results

5.1 Survey of changes in the precipitation climate

To get a general view of precipitation change in the region we present an analysis of the several standard extreme indices (Table 2). The metrics were selected from the ClimDex project (http://www.climdex.org/).

Table 2: Extreme metrics investigated in this project

Long name	**CMIP5/Climdex name**	**Description**
Maximum five-day cumulative precipitation	rx1day	Let RR_{kj} be the precipitation amount for the 1-day interval ending k, period *j*. Then maximum 1-day values for period *j* are: $Rx1day_j = \max(RR_{kj})$
Total annual rainfall when the daily rainfall exceeds the 95th percentile	r95p	Let RR_{wj} be the daily precipitation amount on a wet day *w (RR ≥ 1.0mm)* in period *i* and let $RR_{wn}95$ be the 95th percentile of precipitation on wet days in the 1961-1990 period. If *W* represents the number of wet days in the period, then: $R95p_j = \sum_{w=1}^{W} RR_{wj}$ where $RR_{wj} > RR_{wn}95$

Simple precipitation intensity index	SDII	Let RR_{wj} be the daily precipitation amount on wet days, *w (RR ≥ 1mm)* in period *j*. If *W* represents number of wet days in *j*, then: $SDII_j = \frac{\sum_{w=1}^{W} RR_{wj}}{W}$
Maximum dry spell length	CDD	Let RR_{ij} be the daily precipitation amount on day *i* in period *j*. Count the largest number of consecutive days where: $RR_{ij} < 1mm$
Maximum wet spell length	CWD	Let RR_{ij} be the daily precipitation amount on day *i* in period *j*. Count the largest number of consecutive days where: $RR_{ij} \geq 1mm$

The pattern of precipitation change in the northern hemisphere mid-latitudes is complex. The expectation is that under climate change, precipitation will become more intense because of the increased water holding capacity of the atmosphere (for example, Trenberth *et al*, 2011). Regionally, however, dynamical factors, such as shifts in the positions of the storm tracks and changes in monsoon circulation, complicate this picture. Changes in circulation patterns mean that in some regions, including West Asia and southern Europe, the contribution of increased rainfall intensity to projected annual rainfall totals may be offset by a reduction in frequency of rainy events. This is illustrated by Figure 3, Figure 4 and Figure 5, which show that, in southern Europe and West Asia, precipitation intensity increases universally, whilst the total precipitation reduces in the south and increases in the north - in part due to the projected poleward shift in the mid-latitude storm tracks (Barnes and Polvani, 2013).

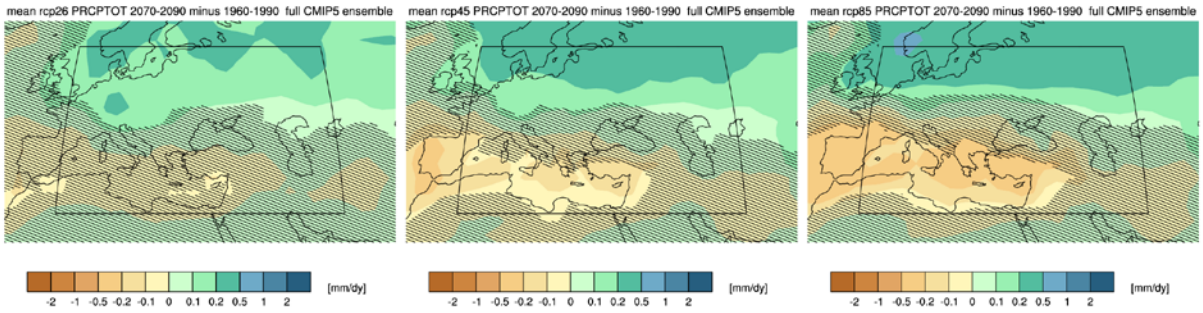

Figure 3: Changes in annual precipitation total for 2070-2090 compared to 1960-1990 for (from left to right) RCP2.6, RCP4.5 and RCP8.5 scenarios. The hatching indicates grid points for which projected changes are smaller than the interannual variability.

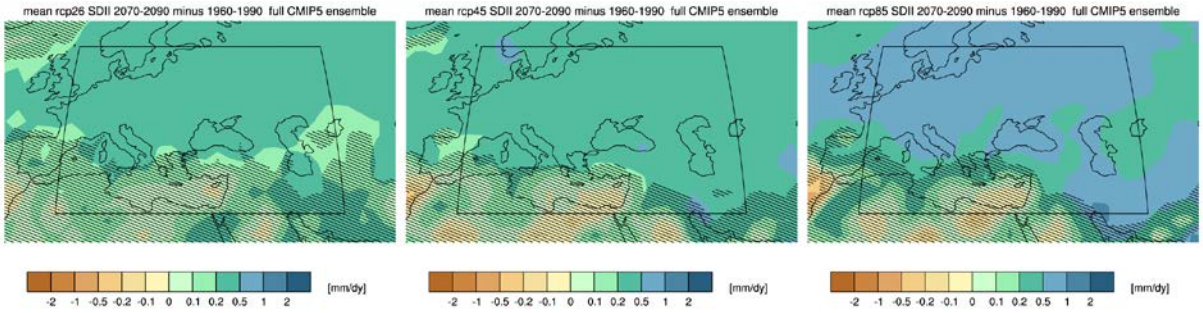

Figure 4: Changes in annual SDII index (rain per rainy day) for 2070-2090 compared to 1960-1990 for (from left to right) RCP2.6, RCP4.5 and RCP8.5 scenarios. The hatching indicates regions where projected changes are smaller than the interannual variability.

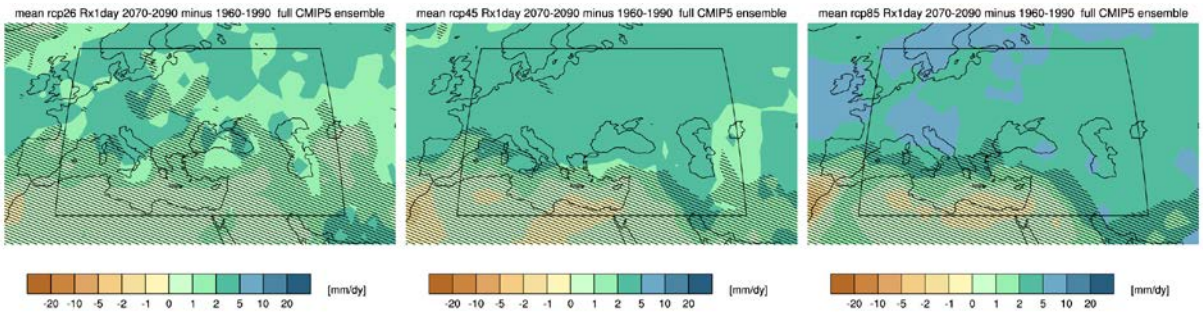

Figure 5: Changes in annual RX1day (annual maximum rainfall on one day) for 2070-2090 compared to 1960-1990 for (from left to right) RCP2.6, RCP4.5 and RCP8.5 scenarios. The hatching indicates regions where projected changes are smaller than the interannual variability.

The projected changes in the duration of dry and wet spells (CDD and CWD) are broadly consistent with this, with increases in the length of dry spells and reduction in the length of wet spells reflecting reduction in the number of rainy days in southern parts of the domain. It should be noted, however, that these metrics are sensitive also to changes in the rainfall seasonal cycle.

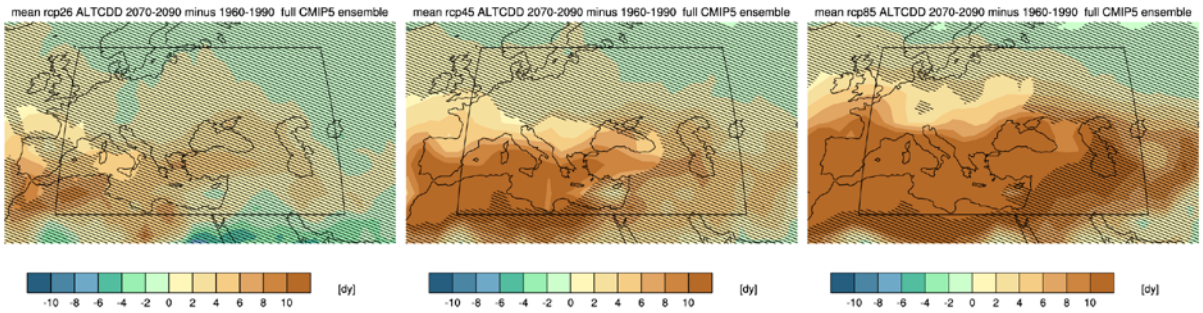

Figure 6: Changes in the annual CDD (length of maximum dry spell) for 2070-2090 compared to 1960-1990 for (from left to right) RCP2.6, RCP4.5 and RCP8.5 scenarios. The hatching indicates regions where projected changes are smaller than the interannual variability.

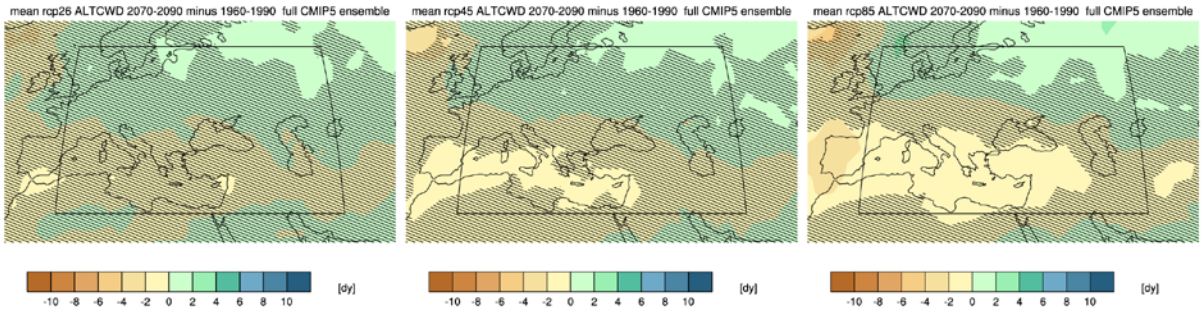

Figure 7: Changes in the annual CWD (length of maximum dry spell) for 2070-2090 compared to 1960-1990 for (from left to right) RCP2.6, RCP4.5 and RCP8.5 scenarios. The hatching indicates regions where projected changes are smaller than the interannual variability.

One effect of increasing intensity is illustrated by Figure 8, which shows that there has been a substantial increase in the amount of annual rainfall falling in high intensity events, even in some parts of the domain that have experienced a reduction in total annual rainfall.

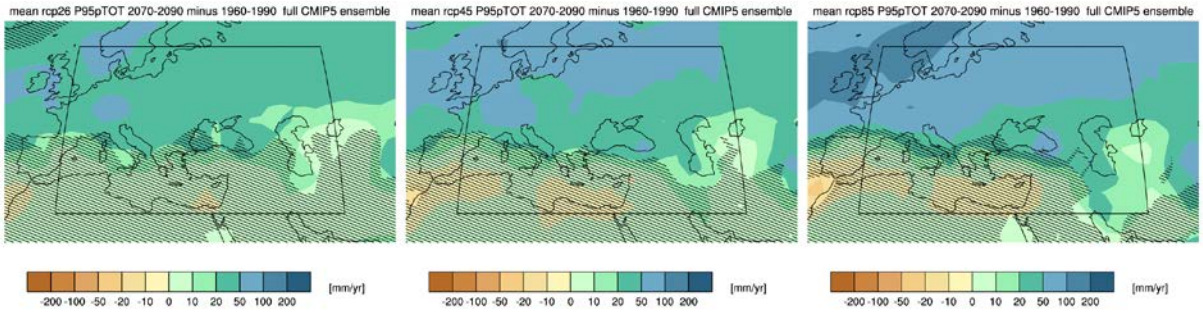

Figure 8: Changes in annual R95p (amount of rain falling during events >95th percentile of rainfall amount) for 2070-2090 compared to 1960-1990 for (from left to right) RCP2.6, RCP4.5 and RCP8.5 scenarios. The hatching indicates regions where projected changes are smaller than the interannual variability.

Time series of changes in rainfall statistics in Georgia (grid box longitude/latitude centred on 44.5^0E, 41.5^0N, 1861-2100) provide insight into the projected evolution of the rainfall climate in Georgia over the next century. Figure 9 shows that there are modest reductions in annual total rainfall in all scenarios by 2030, with significant reduction evident in the RCP8.5 scenario by the end of the 21st Century. Consistent with the previous discussion of regional change, these reductions in precipitation total are accompanied by increases in mean rainfall intensity (Figure 10), reflecting a shift to greater proportions of seasonal rainfall occurring during intense events (Figure 11) and an increase in the maximum rainfall on one day (Figure 12). The subsequent reduction in the number of rainy days is associated with longer dry spells and shorter wet spells (Figure 13 and Figure 14).

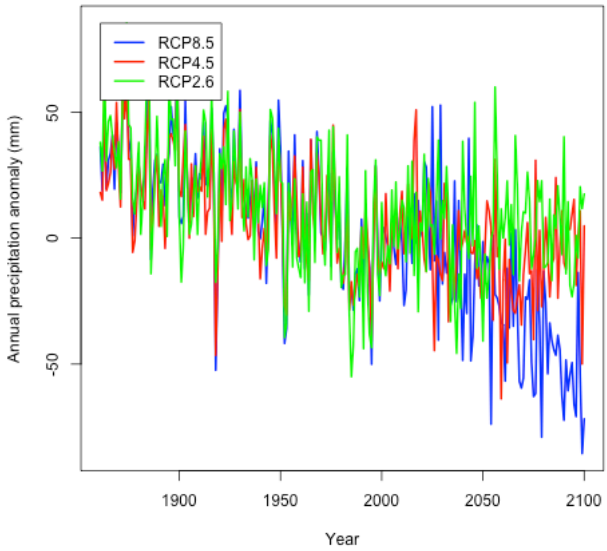

Figure 9: Time series of anomalies in annual precipitation total for three emission scenarios.

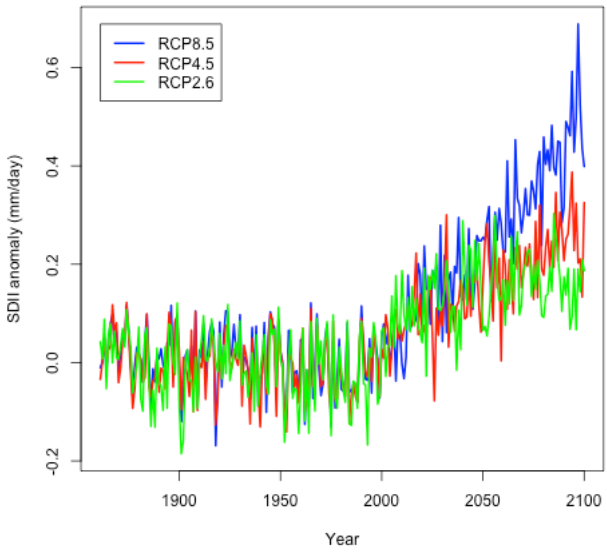

Figure 10: Time series of anomalies in simple intensity index (SDII) for three emission scenarios.

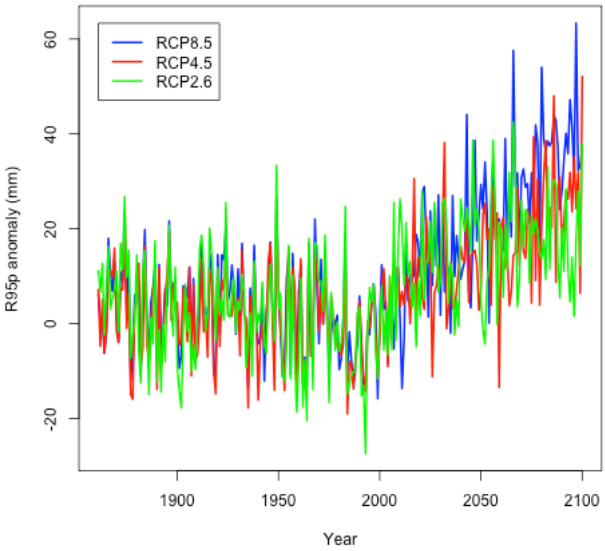

Figure 11: Time series of anomalies in the amount of rain occurring on days with intensity >95th percentile (R95p) for three emission scenarios.

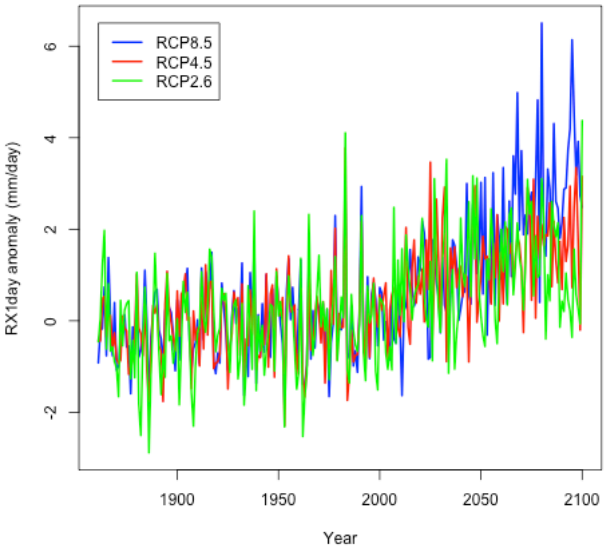

Figure 12: Time series of anomalies in the maximum amount of rain on one day (RX1day) for three emission scenarios.

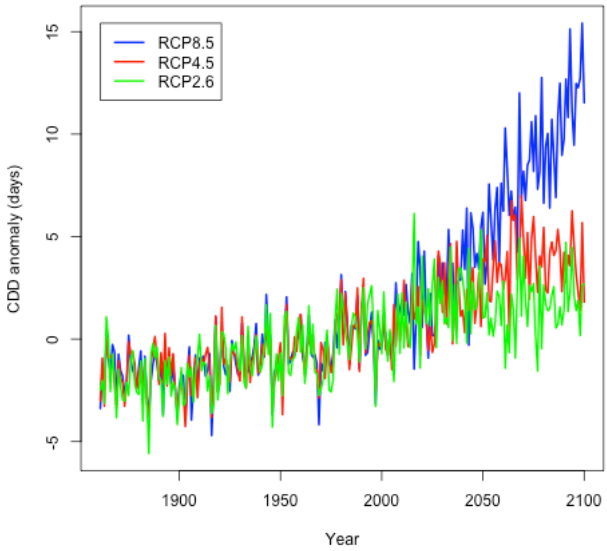

Figure 13: Time series of anomalies maximum length of dry spell (CDD) for three emission scenarios.

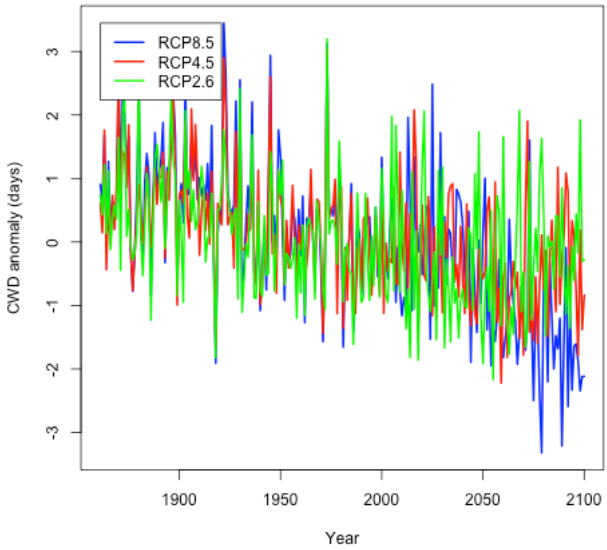

Figure 14: Time series of anomalies maximum length of wet spell (CWD) for three emission scenarios.

Together with previously published analyses of climate change in the mid-latitudes, our survey of changes in the statistics of precipitation tells a coherent story of reduction in rainy events, associated with change in the large-scale pattern of circulation, accompanied by an intensification of rainfall. Significant uncertainties in the magnitude of these changes, however, remain. Firstly, in several cases, there are large differences between the RCP

scenarios - reflecting large scenario uncertainty, especially towards the end of the time series. Secondly, the data are noisy, even in the multi-model mean. The interannual variability for some metrics or regions exceeds the long-term change, as illustrated by the hatching on the maps.

5.2 Return periods of extreme rainfall events

The previous section showed that whilst the total rainfall is projected to reduce in Georgia, the mean intensity of rainfall in projected to increase. The following analyses investigate the net effect of these changes on return periods.

Return periods for extreme rainfall events were derived by fitting a general extreme value (GEV) distribution to the RX1day time slices, using a maximum likelihood approach to estimate the three GEV parameters (broadly following Fowler et al 2007). The changes in return periods based on climate model output were then scaled to the Kojoro gauge data, using a percentile matching approach.

Uncertainty in return periods stems from errors in the GEV distribution parameters for both models and observations, and subsequent errors in the scaling. Because of the non-linearity of the system, we used a Monte Carlo method to infer the confidence intervals on return periods.

Table 3 shows estimated rainfall thresholds for return periods of 5, 25, 50, 100 and 500 years, for both historical observations and for projections, under three climate change scenarios. The results are displayed graphically in Figure 15, Figure 16 and Figure 17.

Table 3: Rainfall thresholds at 5, 25, 50, 100 and 500-year return periods for the historical period and for 2030-2050 and 2070-2090 time slices

Time Slice	Return period (years)	Lower_c.i. (mm)	Median (mm)	Upper_c.i (mm)						
Historical	5	<50	67	85						
	25	85	103	122						
	50	94	121	148						
	100	102	140	178						
	500	115	192	>250						
		RCP2.6			RCP4.5			RCP8.5		
Time Slice	Return period (years)	Lower_c.i. (mm)	Median (mm)	Upper_c.i (mm)	Lower_c.i. (mm)	Median (mm)	Upper_c.i (mm)	Lower_c.i. (mm)	Median (mm)	Upper_c.i (mm)
2030-2050	5	<50	96	160	<50	95	170	<50	97	166
	25	72	136	199	72	147	222	84	153	222
	50	76	146	216	83	161	239	92	171	250
	100	79	153	227	91	171	251	101	183	>250
	500	84	164	243	98	186	274	113	201	>250
2070-2100	5	55	128	202	7	98	189	82	168	>250
	25	81	154	228	84	175	266	113	200	>250
	50	83	160	237	101	188	276	118	205	>250
	100	85	164	242	111	196	282	120	209	>250
	500	89	169	250	122	206	290	123	213	>250

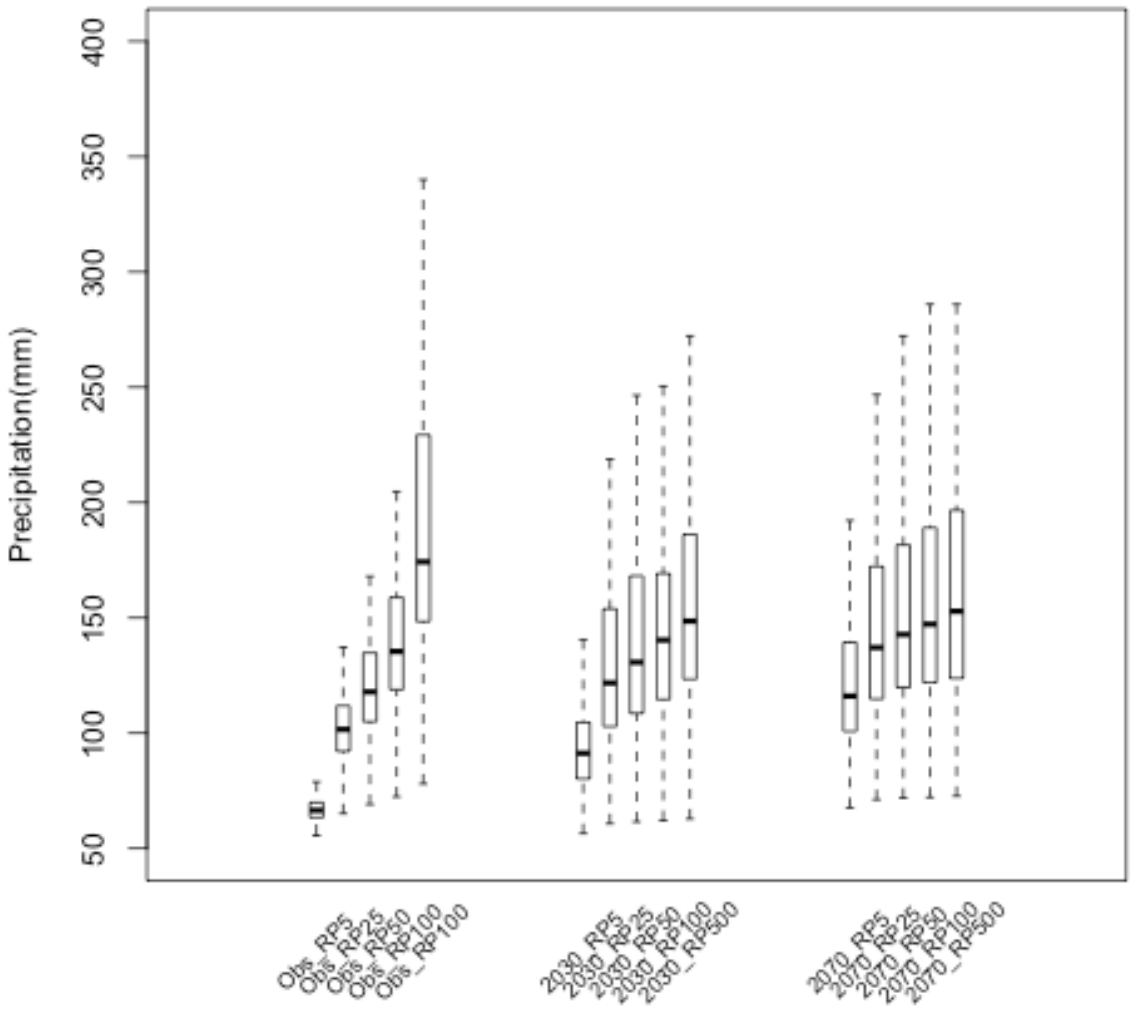

Figure 15: Rainfall for 5, 25, 50, 100 and 500 year return periods for the present day (obs_RP5 etc), 2030-2050 (2030_RP5 etc) and 2070-2090 (2070_RP5 etc) for a RCP2.6 scenario.

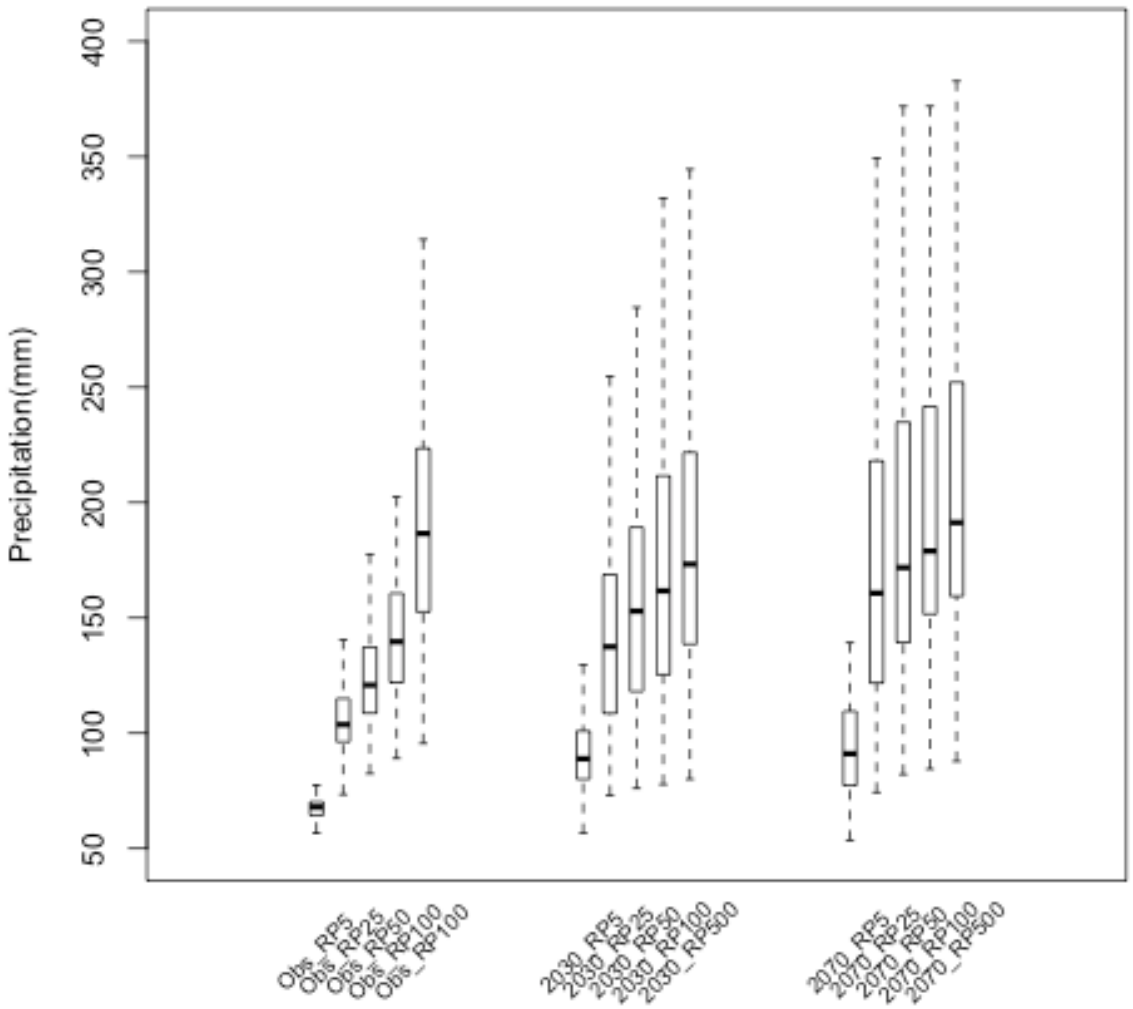

Figure 16: Rainfall for 5, 25, 50, 100 and 500 year return periods for the present day (obs_RP5 etc), 2030-2050 (2030_RP5 etc) and 2070-2090 (2070_RP5 etc) for a RCP4.5 scenario.

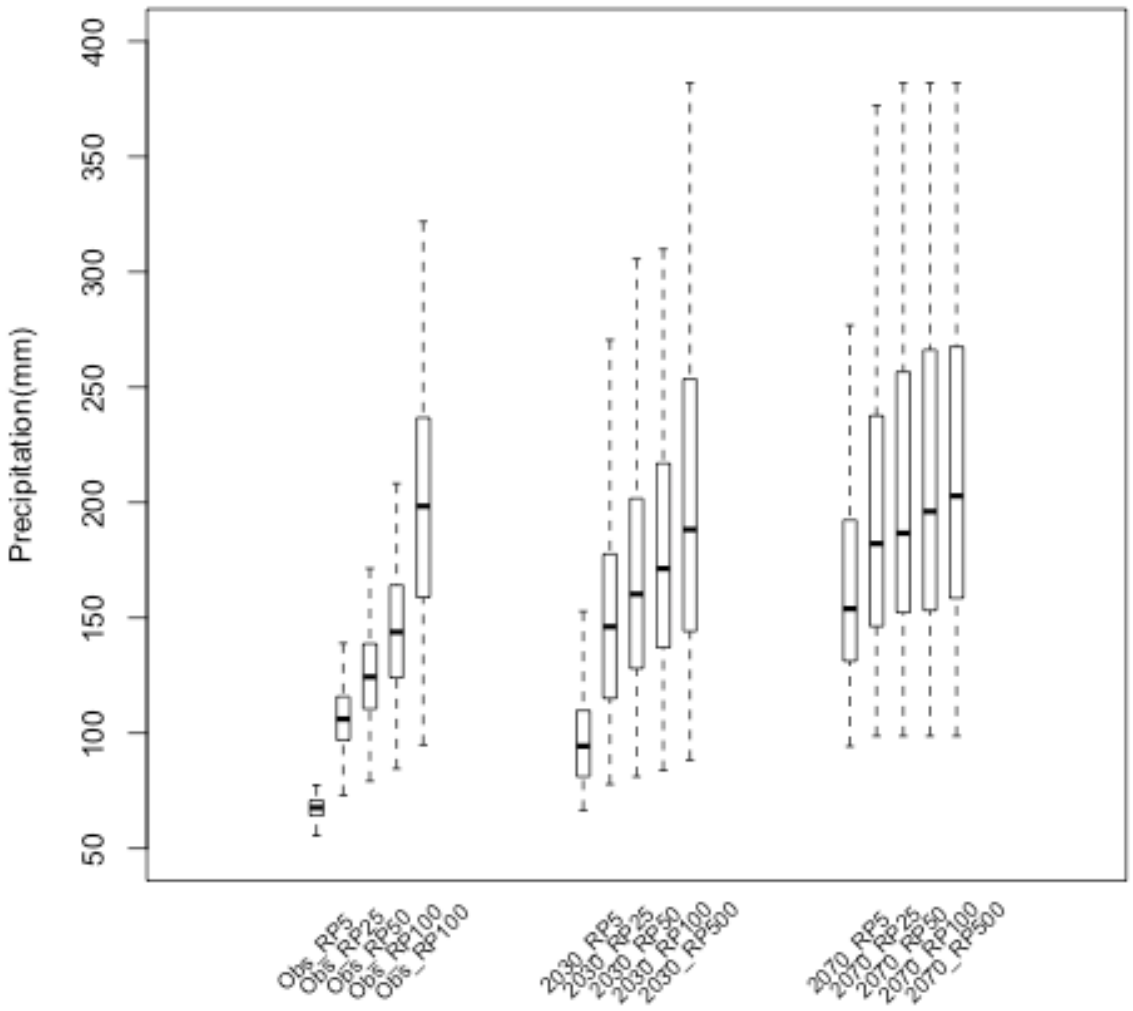

Figure 17: Rainfall for 5, 25, 50, 100 and 500 year return periods for the present day (obs_RP5 etc), 2030-2050 (2030_RP5 etc) and 2070-2090 (2070_RP5 etc) for a RCP8.5 scenario.

Figure 15, Figure 16 and Figure 17 illustrate that the return periods for large rainfall events reduces through time under all scenarios, with the largest changes evident by 2070-2090 for the RCP8.5 scenario. Note that the use of a Monte Carlo method leads to small variations in the 'observed' estimates of rainfall return periods and their confidence intervals in these figure. Although the general patterns in return period are consistent between scenarios, the uncertainties in the exact amount of rainfall for a given return period is large - especially for the long return periods.

6 Conclusions

- Annual rainfall in Georgia is projected to decrease over the 21st centuries under all three RCP scenarios. The daily intensity of rainfall is, however, projected to increase. These findings are generally consistent with previously published work on mid-latitude climate change.
- The net effect of these changes is an increase in rainfall for a given return period - in other words, a reduction in the return period for large rainfall events.
- The uncertainties on the rainfall thresholds are large and stem primarily from the difficulty of estimating the magnitude of rare events from short time series - even using a large multi-model ensemble.

References

Barnes, E.A. and Polvani, L., 2013. Response of the midlatitude jets, and of their variability, to increased greenhouse gases in the CMIP5 models. *Journal of Climate*, *26*(18), pp.7117-7135.

Fowler, H.J., Ekström, M., Blenkinsop, S. and Smith, A.P., 2007. Estimating change in extreme European precipitation using a multimodel ensemble. *Journal of Geophysical Research: Atmospheres*, *112*(D18).

Trenberth, K.E., 2011. Changes in precipitation with climate change. *Climate Research*, *47*(1/2), pp.123-138.

Van Vuuren, D.P., Edmonds, J., Kainuma, M., Riahi, K., Thomson, A., Hibbard, K., Hurtt, G.C., Kram, T., Krey, V., Lamarque, J.F. and Masui, T., 2011. The representative concentration pathways: an overview. *Climatic change*, *109*(1-2), p.5.